Overview of out of plane MEMS assembly techniques.

Michaël Gauthier, Cédric Clévy, Sounkalo Dembélé, Brahim Tamadazte, Kanty Rabenorosoa, Nadine Piat, Philippe Lutz

Overview of out of plane MEMS assembly techniques

M. Gauthier, C. Clévy, S. Dembelé, B. Tamadazte, K. Rabenorosoa, N. Piat, P. Lutz,
FEMTO-ST Institute, UMR CNRS 6174 - UFC / ENSMM / UTBM
Automatic Control and Micro-Mechatronic Systems Department
24, rue Alain Savary, 25000 Besançon, FRANCE
{michael.gauthier ; cedric.clevy ; soukalo.dembele }@femto-st.fr

***Abstract*— This paper deals with a synthesis of the activities of the French FEMTO-ST institute in the field of robotic micro-assembly. It deals with the tridimensional assembly of objects whose typical size is from 10 microns to 400 microns. We are especially focusing on the automation of micro-assembly based on several principles. Closed loop control based on micro-vision has been studied and applied on the fully automatic assembly of several 400 microns objects. Force control has been also analyzed and is proposed for optical Microsystems assembly. At least, open loop trajectories of 40 microns objects with a throughput of 1800 unit per hour have been achieved. Scientific and technological aspects and industrial relevance will be presented.**

I. Introduction

Until now, miniaturization was driven by a general diminution of the volume of the product (e.g. cell phones). Currently, the major objective of the miniaturization is to increase the number of functionalities in a product whose volume is mostly constant (e.g. smart phone). In the future, the functions realized using micro or nanotechnologies would be assembled and packaged in order to build integrated multifunctional products or even intelligent products. The hybridization of technologies in micronanosystems is consequently a major stake for the next ten years.The application fields of these future products are typically the networks of sensors for environmental monitoring or the diagnostic and drug delivery done by intelligent systems embedded in human body.

Industrial robotics at this scale should be especially studied in order to propose handling, positioning solutions for automatic assembly of these new generation systems. The study of micronanomanipulation strategies deals with handling and positioning of objects whose typical sizes are from 1nm to 1mm. The particularity is that it is covered a high range including 6 orders of magnitude. The performances of academic and industrial robots strongly depend of the scale considered in these 6 orders of magnitude which consists in several technological and scientific problematics. During the last ten years, micromanipulation solutions down to 50 micrometers have been proposed in academic institutes (participant of this workshop). They currently are able to be applied in industries in the field of scientific instrumentation, in the assembly of miniaturized mechatronics or mechanical systems (Percipio Robotics, Watch industries, medical devices), and also in microelectronics (NXP, ST microelectronics, Beam Express) with the advent of tridimensional components (3D-STACK).

This paper summarizes the activities of the French institute FEMTO-ST in micromanipulation and micro-assembly. First section is presented automatic 3D assembly using visual sevoing on 400 microns objects. An other way to assemble automatically microparts is to use force control as presented in the next section. Teleoperation of the assembly 40 microns objects are going to be related in section IV before a presentation of the future challenges in micronanoassembly.

II. 3D microassembly using visual servoing

The objective of the research is the assembly of microparts by inserting them into each other by means of 3D visual servoing. Thanks to the precision of the latter one hopes to obtain solid 3D MEMS without any solidaring effect.

The parts involved in the experiments measure $400\mu m \times 400\mu m \times 100\mu m$, the grooves measured $97\mu m \times 97\mu m \times 100\mu m$. Every micropart is etched with a precision of $\pm 1\mu m$, therefore, the assembly clearance of two microparts ranges between 1 μm and 5μm (figure 1).

Let **A** and **B** be two microparts to assemble, the objective is then to automatically insert a groove of **A** into a groove of **B**. The problem is divided into three basic tasks that should be performed in the following sequence: the positioning of **A** at the assembly place (task#1), the positioning of **B** at the insertion place (task#2) and the vertical insertion of **B** into **A** (task#3) (figure 1).

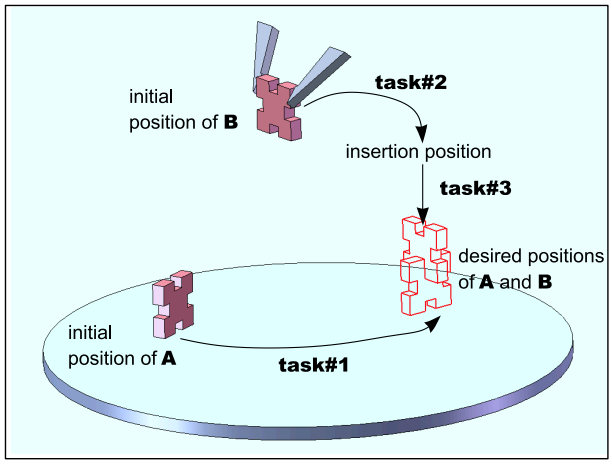

Fig. 1. Objective of the work: insertion of two microparts by their groove

Let R_c,R_A, R_{A*}, R_B and R_{B*_2} be the frame attached to the camera (i.e. the videomicroscope), the current and final frames of the micropart **A**, the current and final frames of the micropart **B**, respectively. Moreover, an insertion frame (R_{B*_1}) for **B** is required where the part process through before switching to the insertion stage (2).

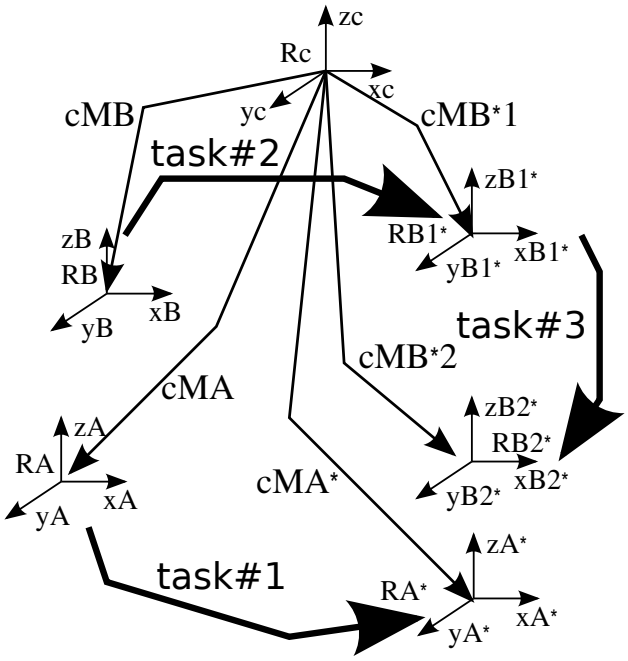

Fig. 2. Diagram of the insertion of part **B** into **A**

A CAD model of the microparts based tracking from ([1]) is used. It provides, for each new image, the following information:

- ${}^c\mathbf{M}_A$, the homogeneous transformation between the camera frame and the current position of **A**,
- ${}^c\mathbf{M}_B$, the homogeneous transformation between the camera frame and the current frame of **B**.

Let

- ${}^c\mathbf{M}_{A*}$ be the homogeneous transformation between the camera frame and the desired frame of **A**,
- ${}^c\mathbf{M}_{B*_1}$ be the homogeneous transformation between the camera frame and the insertion frame of **B**,
- ${}^c\mathbf{M}_{B*_2}$ be the homogeneous transformation between the camera frame and the desired frame of **B**.

Every task is achieved as followed:

- task#1: displacement of the micropart **A** to a given position (defined by R_{A*}); the achievement of this task is ensured by a control law regulating to zero the error defined as:

$$ {}^A\mathbf{M}_{A*} = {}^c\mathbf{M}_A^{-1}.{}^c\mathbf{M}_{A*} \tag{1}$$

- task#2: displacement of the second micropart **B** to an intermediate position (defined by R_{B*_1}) whose achievement is ensured by a control law regulating to zero the error defined as:

$$ {}^B\mathbf{M}_{B*_1} = {}^c\mathbf{M}_B^{-1}.{}^c\mathbf{M}_{B*_1} \tag{2}$$

- task#3: insertion of micropart **B** in micropart **A** (defined by R_{B*_2}) whose achievement is ensured by a control law regulating to zero the error defined as:

$$ {}^B\mathbf{M}_{B*_2} = {}^c\mathbf{M}_B^{-1}.{}^c\mathbf{M}_{B*_2} \tag{3}$$

The switching between task#2 and task#3 is done when the error reached a predefined level. The microparts desired poses ${}^c\mathbf{M}_{A*}$, ${}^c\mathbf{M}_{B_1}$ and ${}^c\mathbf{M}_{B_2}$ are obtained either in teleoperated mode (using a joystick) or directly from the CAD model. The accurate definition of R_{B*_1} is important for the success of the insertion.

Let R_F be the base frame of the workcell. The homogeneous transformation between the camera frame R_c and the workcell frame R_F is noted ${}^F\mathbf{M}_A$ and is computed for each object pose.

For each task the regulation to zero of the error $\mathbf{e}$ defined from ${}^i\mathbf{M}*_i$ consisted of choosing $s = ({}^Ft_i, \theta u)$ as the current 3D pose and $s* = ({}^Ft_{i*}, 0)$ as the desired pose of the micropart i, respectively:

$$ \mathbf{e} = \begin{pmatrix} {}^Ft_i - {}^Ft_{i*} & \theta u \end{pmatrix} \tag{4}$$

The corresponding control law defined by the exponential decrease of the error is then:

$$ \begin{pmatrix} v \\ \omega \end{pmatrix}_F = -\lambda \begin{pmatrix} \mathbf{I}_{3x3} & \mathbf{0}_{3x3} \\ \mathbf{0}_{3x3} & \mathbf{J}_\omega^{-1} \end{pmatrix} (s - s*) = -\lambda \begin{pmatrix} {}^Ft_i - {}^Ft_{i*} \\ {}^F\mathbf{R}_i \theta u \end{pmatrix} \tag{5}$$

The task 1 involves the control of the xyα table as:

$$ \begin{pmatrix} v_x \\ v_y \\ \omega_\alpha \end{pmatrix}_F = -\lambda_1 \begin{pmatrix} {}^Ft_x - {}^Ft_{x*} \\ {}^Ft_y - {}^Ft_{y*} \\ {}^F\mathbf{R}_A \theta u_\alpha \end{pmatrix} \tag{6}$$

The task 2 involves the control of the xyα table as:

$$ \begin{pmatrix} v_x \\ v_y \\ \omega_\alpha \end{pmatrix}_F = -\lambda_2 \begin{pmatrix} {}^Ft_x - {}^Ft_{x*} \\ {}^Ft_y - {}^Ft_{y*} \\ {}^F\mathbf{R}_B \theta u_\alpha \end{pmatrix} \tag{7}$$

The task 3 involves the control of the zϕ manipulator as:

$$ \begin{pmatrix} v_z \\ \omega_\phi \end{pmatrix}_F = -\lambda_3 \begin{pmatrix} {}^Ft_z - {}^Ft_{z*} \\ {}^F\mathbf{R}_A \theta u_\phi \end{pmatrix} \tag{8}$$

The terms λ, λ_1, $\lambda_2$and λ_3 are the gains enabling the modulation of the decrease speed.

A. experimental set-up

The setup includes a robotic system in combination with a microhandling and an imaging systems (figure 3). It is positioned inside a controlled environment on a vibration-free table. Two PCs connected by an Ethernet link processes the information, the first (Pentium (R) D, CPU 2.80 G Hz, 2 Go of RAM) is dedicated to vision algorithms while the second (Pentium (R) 4, CPU 3.00 G Hz, and 1 Go of RAM) is used for the control algorithms running. From a kinematic point of view, the workstation is a five DOF robotic system. Three DOF in translation are achieved by three high accuracy linear stages and two DOF in rotation are achieved by two high accuracy angular stages (all from Polytec PI). The five DOF are distributed into two robotic

systems: a xyα system and a zϕ system. The former system (positioning table) is equipped with a compliant support and enables the positioning of parts in the horizontal plane. The latter system (manipulator) supports the gripper and enables the vertical positioning and spatial orientation of microparts. The microhandling system is a two-finger gripper with four DOF (two per finger) developed in the department ([2]). It enables open-and-close motions as well as small up-and-down motions. Every finger is a piezoelectric bimorph with an end-effector made of silicon layers ($12\mu m$ and $400\mu m$) separated by an oxide layer ($1\mu m$). Modularity is an important design criterion during development, so the microgripper has been designed in order to use different end-effectors (finger tips). Thus, it can grab a high variety of objects according to the type of end-effectors used: planar silicon microparts, balls, gears, optical fibers, etc. The sample used in the current experiments is endowed with nickel end-effectors. The corresponding characteristics and performances are summarized in Table 2. The imaging system comprises two photon videomicroscopes. The first one is a LEICA MZ16A that delivers vertical images of the scene, but is not used in the current experiments. The second is a CCD camera associated with a $11.452mm$ focal-length lens and a $140mm$ optical tube. It is positioned at an angle of $\pi/4$ rad from the horizontal plane in order to ensure the best perspective view during the assembly tasks. The image format is $1280 \times 960 pixels$. The other specifications include: a resolution of $0.95\mu m$, a working distance of $80mm$, a field-of-view of $1.216mm \times 0.912mm$ and a depth-of-field which varies between $0.09mm$ to $0.98mm$ with respect to the magnification value. According to the references [3], [4], [5] and [6] this videomicroscope can be described by the linear perspective model whose parameters are the scale factor, the focal-length, the position of the principal point. A 2D calibration template is used to identify these parameters.

Fig. 3. Assembly setup: (a) global view, (b) robotic system, (c)table and gripper, (d) microscope used, (e) gripper with nickel end-ef fectors

B. Results

Figure 4 shows some snapshots taken during the insertion (the CAD model is reprojected onto the micropart) and figure 5 shows some SEM (scanning electron microscope) images of the final assembly.

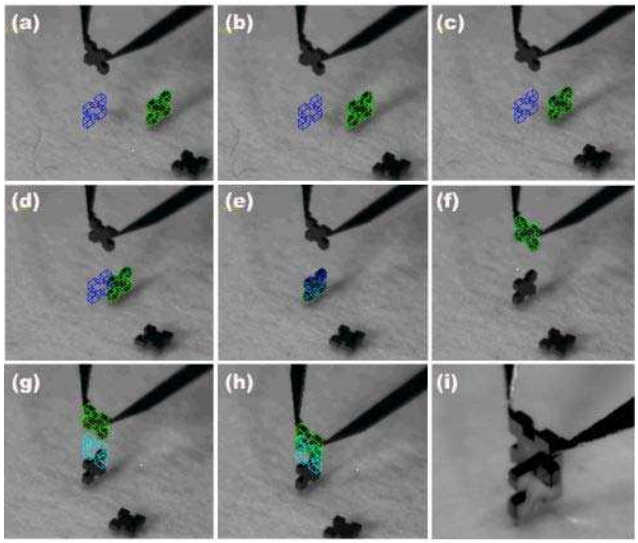

Fig. 4. Some images of the assembly process

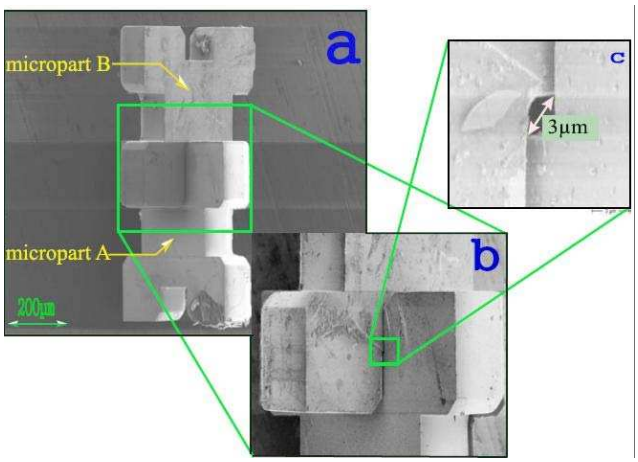

Fig. 5. Some images of the assembled structure from a scanning electron microscope

The strengths of the assembly approach are the precision, the robustness and the speed of processing. Figure 6 shows the evolution of the error e_x, e_y and e_α versus the number of iterations i. The final positioning error along x and y axis of the micropart **A** (task#1) are e_x = 3.52 μm and e_y = 0.29 μm, respectively. The final orientation error in the same task is $e_\alpha = 0.30 \times 10^{-2}$ rad. Figure 7 shows the evolution of the errors e_z and e_ϕ versus the number of iterations i. The final positioning error along z axis of the micropart **B** is e_z = 2.28 μm and the final orientation error e_ϕ with respect to the vertical axis, in the same task, is $e_\phi = 0.13 \times 10^{-2}$ rad. These values are estimated from the encoders of the various angular and linear motions and the kinematic model.

Figure 8 represents the micropart trajectories during the achievement of the different assembly tasks as shown in figure 2. It can be noted that the previously proposed 3D control law achieves, as expected, a straight line trajectories of the

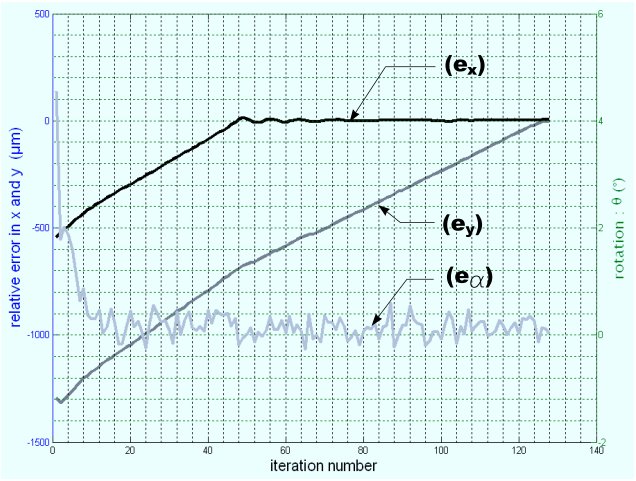

Fig. 6. Positioning error of the table.

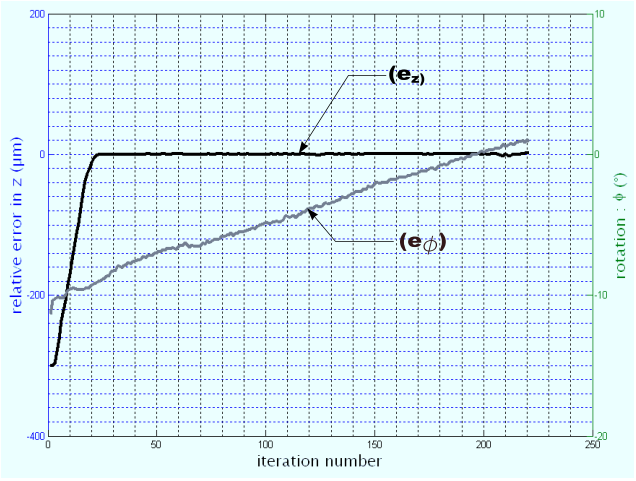

Fig. 7. Positioning error of the manipulator.

microparts. This is especially visible for the displacement of the micropart A located on the 3 DOF positioning platform.

Regarding the robustness, the approach works despite partial occlusions of parts and the blurred images (because of the small depth of field of the microscope). The assembly is performed successively 10 times, it takes an average of $41s$ with a standard deviation of $3s$.

Those interesting specifications of the developed assembly approach lead us to try the assembly of a complex structure: the assembly of 5 microparts (**A**, **B**, **C**, **D**, **E**) on three levels. Figure 9 shows the result: a right and stable structure is obtained without any use of solidaring effect.

The concepts developed here, the assembly of MEMS by means of visual servoing, have been validated with parts measuring $400\mu m \times 400\mu m \times 100\mu m$. The grooves have been measured $97\mu m \times 97\mu m \times 100\mu m$ with an assembly clearance ranging from $1\mu m$ to $5\mu m$. But they can be extended to parts of smaller dimensions since the tracking of $40\mu m \times 40\mu m \times 5\mu m$ under a scanning electron microscope has been possible (figure 10).

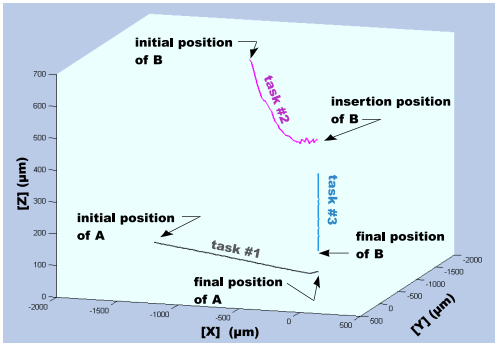

Fig. 8. Part trajectories.

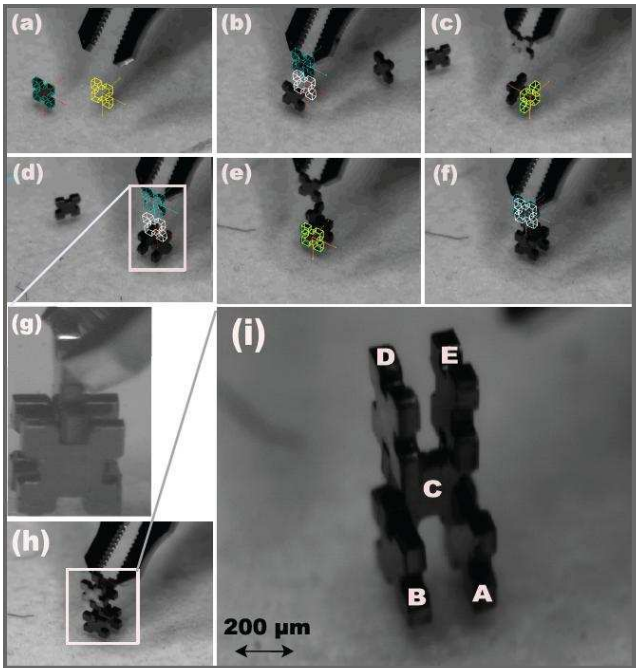

Fig. 9. Assembly of five parts on three levels.

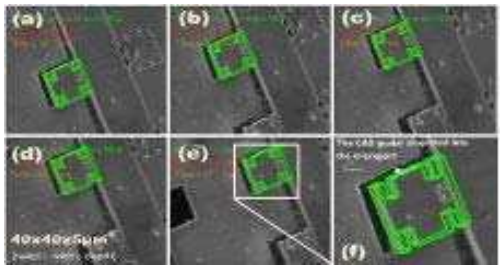

Fig. 10. Tracking of a small part in the images from a scanning electron microscope.

III. Microassembly of MOEMS using force control

Scale effects largely influence the yield and complexity of micro-assembly processes. For example, surface forces are predominant at the microscale whereas surface contacts often happen during micro-assembly processes (contact between gripping tool and components to manipulate, contact between several components to assemble, contact between one component and its environment...). Surface forces have been widely studied but mainly at the "nanoscale" through contact points but very few investigation have been performed to model or quantify these forces at the microscale and for planar contacts. Among first studies, it was shown that pull-off forces (force required to separate two components in planar contact) may reach 200 μN for 50x50 μm^2 Silicon surface contact [7]. The lack of measurement and models to characterize contact forces happening during micro-assembly process combined with their strong influence lead to the need to integrate force sensing capabilities during micro-assembly processes. Despite this important need, the integration of force sensors within micro-assembly stations remains highly challenging because it requires to design and fabricate sensors with suitable measurement range, resolution, bandwidth and small enough size at the same time [8]. Based on these statements, this section will shortly introduce one application requiring contact force measurement during micro-assembly process. The integration of innovative force sensors within the corresponding micro-assembly workstation will then be displayed. Finally, results about hybrid force/position control applied to guiding micro-assembly tasks will be given.

A. Application

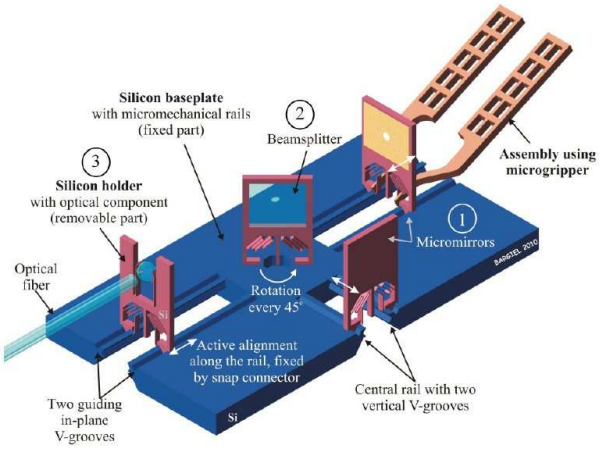

Fig. 11. Principle of RFS-MOB: A microgripper pick and place holders on a baseplate. In this example, 4 holders (2 mirrors, one with ball lens and one beam splitter) are placed on the baseplate. Fine positioning of holders on the baseplate is ensured due to guiding rails [9].

The concept of RFS-MOB (Reconfigurable Free Space Micro-Optical-Benches) is developed within the FEMTO-ST Institute (see Fig. 11). Generic components (named holders) comprise optical functionalities; they integrate, for example, a micromirror, a ball lens, a beam splitter, a laser emitter or a sensor. These holders are assembled on a unique baseplate to constitute one product. It's thus possible to fabricate products like microspectrometers, confocal microscopes...The size of holders is 1200x800 μm^2 enabling highly integrated solutions. Details about this concept are displayed in Fig. 11 and in [10].

Holders are combined together depending on the targeted application. Based on basic holders, optical functionalities and baseplates, it's possible to fabricate a wide variety of assembled products enabling complex functionalities and Free Space out of plane optical path. Fig. 12 displays a basic example of RFS-MOB.

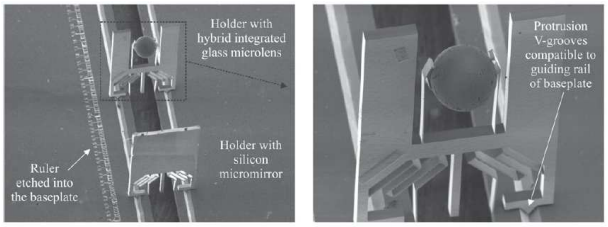

Fig. 12. Example of RFS-MOB comprising 2 holders (one mirror and one ball lens holder) on a baseplate [10]. The ball lens is 258 μm in diameter.

The assembly of holders onto the baseplate constitute one of the main challenging tasks to fabricate these RFS-MOB. This task has to enable the positioning of each holder at the good location with the required positioning accuracy: in most cases, better than 1 μm to ensure the optical performances of the assembled product. This delicate task is done using a microgripper to handle the holder (see Fig. 13). A guiding task is then performed to ensure the positioning of the handled holder into a guiding rail. Once the suitable position is reached, the microgripper is opened releasing the holder. Springs of the holder then apply a force onto the baseplate that ensures the holding of the position of the holder relative to the baseplate.

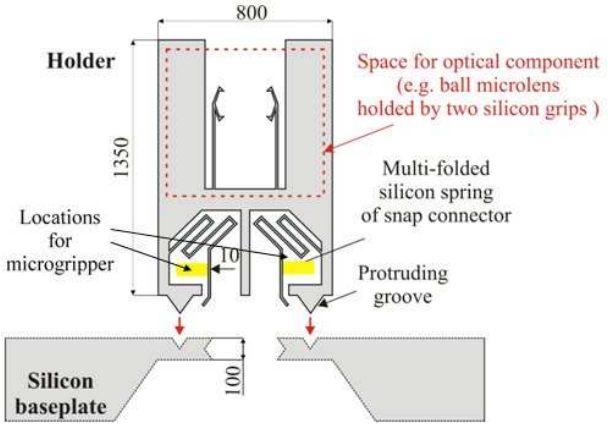

Fig. 13. Holders are handled using a microgripper. Both fingers of the microgripper apply a force on the springs of holder [10].

B. Experimental set-up

The guiding of the holder onto the rail and its releasing are the most delicate assembly task for several reasons:

- manipulated holders are flexible making the handling possibly unstable,
- when a contact between the holder and the guiding rail happens, the presence of pull-off force is source of instabilities during the guiding,
- imperfections of the micro-assembly platform's kinematic make difficult to achieve guiding tasks based on position control.

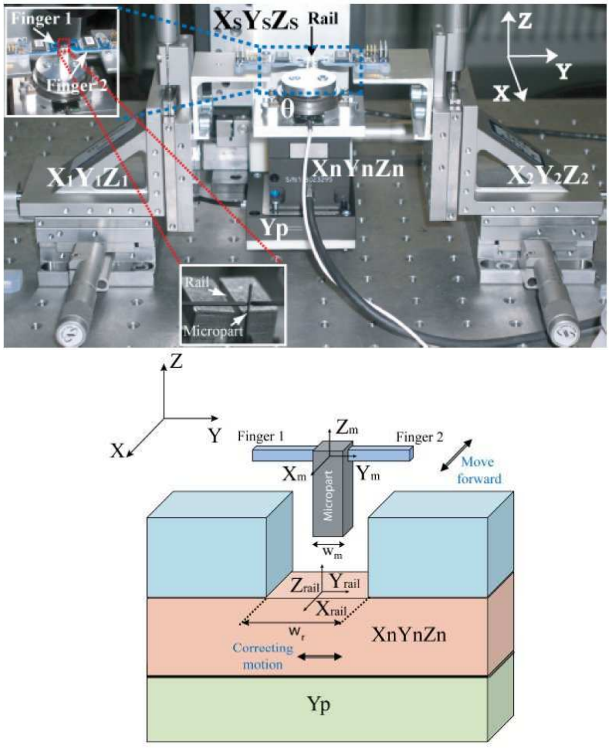

Fig. 14. Photo and principle scheme of the experimental set-up used for achieving hybrid force-position controlled guiding tasks. The component to guide into the rail is hold by a microgripper comprising two independently controlled fingers. The rail can be moved by $X_nY_nZ_nY_p$ motions [11].

To achieve micro-assembly tasks such as guiding or insertion, the combination of force and position control thus constitutes a promising approach. An experimental set-up has been developed to study such tasks and methodologies (Fig. 14). It is based on two fingers that can be independently controlled to achieve gripping tasks. Each finger integrates one force sensor sold by Femtotools (+/- 2mN of measuring range) enabling to measure the force applied by the finger on the handled component. We consider microcomponents of 2mm long with 50x50 μm^2 of cross-section. Each finger is also mounted on a 3D structure (XYZ) to generate translations. Thus, the gripping of the component can be ensured and force controlled. Once the component gripped, both fingers can be moved together to ensure the guiding of the component into a rail. During this guiding:

- the gripping force is kept constant,
- contacts between the gripped component and the rail have to be detected the fastest possible to prevent from breaking or loosing the gripped component,
- contacts between the gripped component and the rail have to be quantified (through measurement) to perform the suitable motions to remove or limit the contact (required to achieve the guiding without breaking or loosing the component).

The objective of the guiding task relies in moving the gripped component into the rail along the X axis (in the present case, see Fig. 14 and to position it at the required location. Thus, the motion along X will be controlled in position. When a contact between the gripped component and the rail happens, a force along Y is measured. Motion along Y are so generated to reduce these forces, thus the Y axis will be controlled in force. The combination of both of these controls lead to hybrid force position control. The control scheme that is applied is given in Fig. 15.

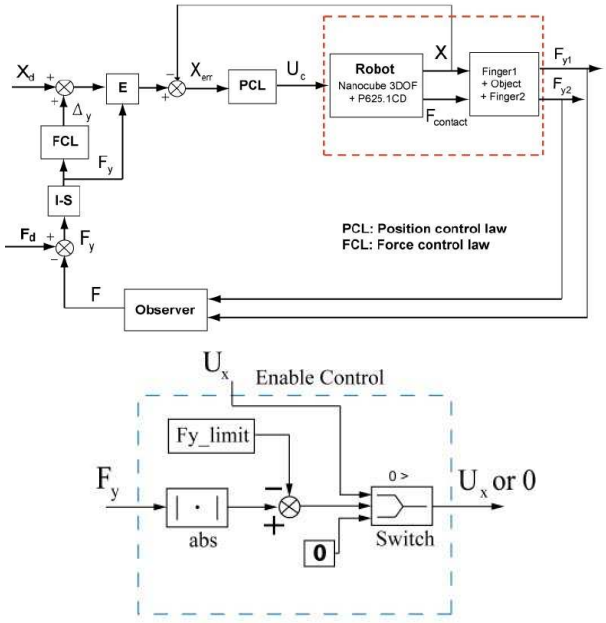

Fig. 15. Hybrid force control scheme used to achieve automated guiding tasks and details about the Enable control block E [11].X_d is the input position, F_d the input force, S selection matrix, FCL the Force control law, PCL the position control law and F the estimated contact force between the gripped component and the rail.

C. Results

The platform and hybrid force-position control law described above have been used and applied to achieve automated guiding tasks at the microscale. The integration of 2 force sensors for microscale grippers enabled to understand several phenomena that was up there not identified due to too small scale and lack of sensors. First, pull-off force for planar contact of 50x50 μm^2 has been measured for the first time. It showed that such force may reach up to 196 μN of amplitude and to identify the most influent parameters. Results are detailed in [7]. Secondly, the detailed motions of the gripped component have been identified during when an external contact force is applied. Two main steps have notably been determined (see details in Fig. 16):

- when a small lateral external force is applied on the gripped component, the contact between the component

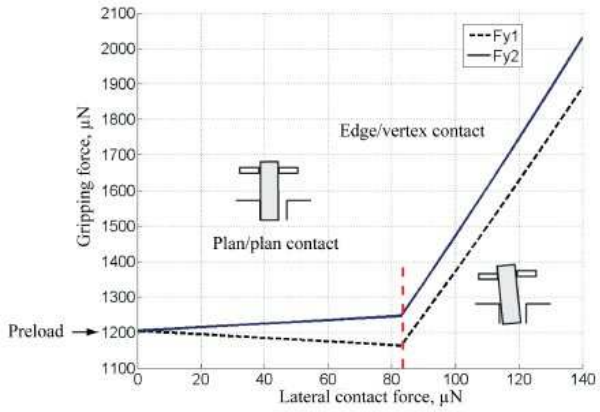

Fig. 16. Gripping force versus external lateral contact force evolution showing 2 steps: once the preload applied, the contact between gripped component and fingers of the microgrippers remains planar (good stability of the grasping). Once the lateral contact force reach 85 μN, the component rotates (edge/vertex contact) decreasing a lot the stability of the grasping [12].

and fingers of the microgripper remains planar which ensure a good stability of the grasping,

- when the lateral contact force passes a limit which depends on the preload force and several geometric parameters, the fingers of the microgripper used to bend, generating a rotation of the component. Thus, edge/vertex contacts happen between the gripped component and the microgripper reducing a lot the stability of the grasp.

The developed experimental platform enabled to identify this behavior but also to obtain and validate a fine behavioral model of the microgripping (see details like studies of influent parameters and experimental validation in [12]).

Based on this model, a simulator has been developed in order to simulate automated guiding tasks, choosing the controller and setting up his parameters. Indeed, experimentations remains extremely challenging at this scale making simulation of great help. Controller and set parameters have then been implemented on the experimental platform. An incremental controller has been chosen as a first step for his simplicity, efficiency and robustness.

Automated guiding tasks have been experimentally performed based on incremental force controller. It enabled to achieve such tasks despite the possible presence of pull-off forces. The response time for reduction of perturbation under a given value (15 μN in the present case) is off 35 ms (see Fig. 17). This experimental set-up enabled to validate the efficiency of hybrid force-position control at the microscale to achieve automated guiding tasks. Future works will be done to focuss on several degrees of freedom tasks such as insertion.

IV. Teleoperated assembly of 40 microns objects

The last category of works deals with smaller object whose size is between 10 to 100 microns. At that scale adhesion cannot be neglected and should be taken into account in the design of handling strategies. We are proposing a new

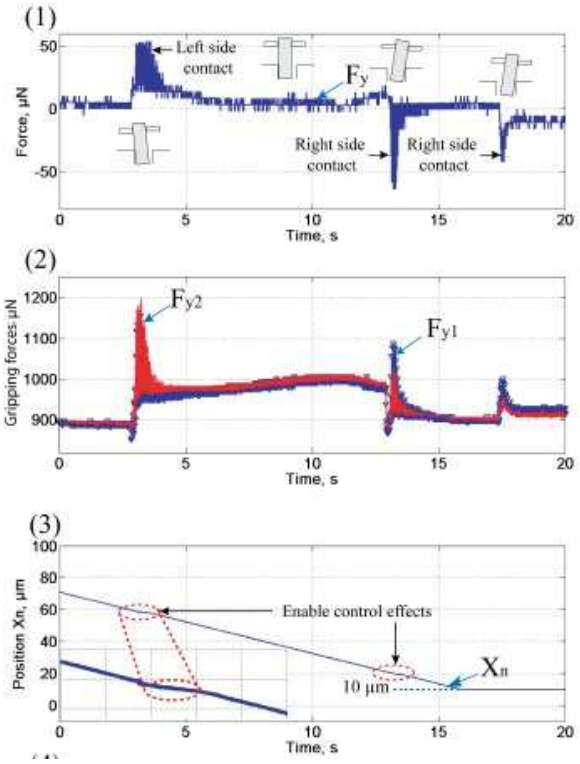

Fig. 17. Experimental results of a guiding task (1) lateral contact force estimation (2) gripping force evolution for left side and right side contact (3) move forward motion.

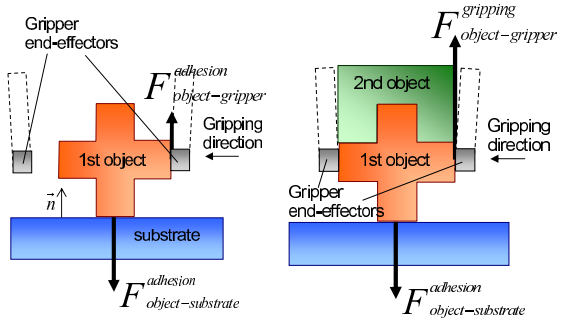

(a) Releasing the first object on the substrate

(b) Grasping the first object from the substrate

Fig. 18. Principle of the Release and Grasping of the First Object

reliable and reversible method to position micro-object on a substrate. The principle is an hybrid strategy between adhesion manipulation and gripping. It is based on a hierarchy of forces. In one hand, to guarantee object's release, the adhesion force between object and substrate must be higher than the adhesion force between object and gripper along the normal vector $\vec{n}$ of the substrate (see in figure 18(a)):

$$F^{adhesion}_{object-substrate} \gg F^{adhesion}_{object-gripper} \quad (9)$$

To reduce the impact of external perturbations, $F^{adhesion}_{object-gripper}$ must be lower as possible and $F^{adhesion}_{object-substrate}$ must be higher as possible. The major drawback of this release method is the difficulties to grasp

the object on the substrate [13]. A reliable grasping cannot be obtained by using only the adhesion force of the gripper. This method is a good way to release the object but not for grasping.

In other hand, to grasp the object, a gripping force higher than the adhesion force between substrate and object along the direction $\vec{n}$ is required (see in figure 18(b)):

$$F^{gripping}_{object-gripper} \gg F^{adhesion}_{object-substrate} \quad (10)$$

One of the best technological solution is to use gripper with two fingers where the gripping force could be easily higher than adhesion between the object and the substrate.

Our hydrid method uses advantages of both adhesion manipulation and gripping. It induces a reliable release and grasping of micro-object. To guarantee, the conditions (9, 10), the gripper must have a high ratio between its gripping force and the adhesion force 'object-gripper'.

As presented in figure 18, two ways have been chosen to guarantee first object's manipulation: increase adhesion forces between the substrate and the object and decrease adhesion force between the object and the gripper.

We chose to use as substrate a transparent gel film well-known in microelectronics: Gel-Pak. This material is in fact transparent and softly adhesive, it consequently allows accurate pick and place tasks. Moreover, the low mechanical stiffness of this polymer induces natural compliance of the substrate required for micro-assembly. In a second time, efforts have been made on end-effectors shaping. First, surface in contact with the micro-object has been reduced by using end-effectors with a small thickness. In second time, the fabrication process called DRIE have been used to give the gripping surface a specific texture. Etching anisotropy of this process is made by a short succession of isotropic etching/protection cycles. These cycles create a phenomenon called *scalloping* illustrated in figure 19. In this way, contact shape between object and end-effectors is a succession of microscopic contact points. The roughness induced by DRIE is able to highly reduce pull-off force. As presented in figure 20, nanostructurations or chemical functionnalisations can also be used to reduce the adhesion on the gripper end-effectors [14], [15], [16], [17].

A. Experimental set-up

The experimental set-up is based on the piezoelectric gripper presented above. Several kind of finger tips can be glued on this piezoelectric actuator. The finger tips[18], [19] used for micro-assembly have been designed to handle microscopic objects. They are build in single crystal silicon SOI wafer by a well-known microfabrication process: DRIE. These end-effectors have a long and thin beam (12 μm) designed to handle objects from 5 μm to few hundred micrometers.

Testing micro-assembly needs micro-objects that could be mechanically fastened to the others. Thus, micro-objects have been designed with mechanical fastener structures already studied in[20]. To supply a challenging benchmark, objects' shape are squares of 40 μm sides with a thickness of 5 μm.

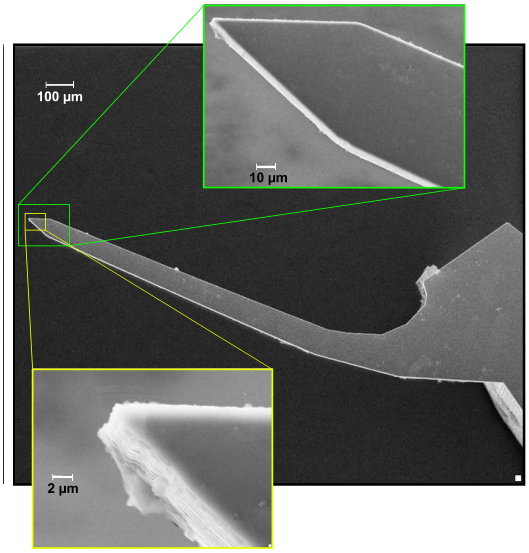

Fig. 19. End-effectors' shape in SEM view. Scalloping is visible in lower picture.

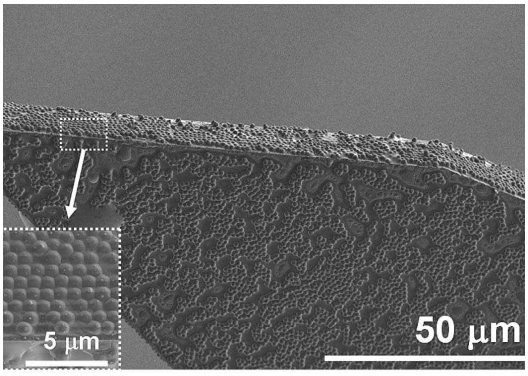

Fig. 20. Nanostructuration of End-effectors' shape (collaborative works between FEMTO-ST and EMPA Institute, Thun, Switzerland) [17]

SOI wafers of 5 μm device layer thickness and DRIE process have been used to build these microparts [21]. Many shapes, fastener designs and sizes were tested (figure 21). Two kind of parts are presented in this article: the first one is 40 μm square puzzle parts, with four notches of 5 μm. The second one is a mechanical plug device between two 40 μm squares. The male part have a key which is able to lock the female part after assembly as proposed by Dechev[20].

B. Results

This approach has been tested in teleoperate mode to assemble benchmark micro-objects. Two kind of mechanical assembly have been tried to make a three-dimensional micro-product. The first one is made by an insertion of two identical puzzle parts. The second one is a reversible assembly of two different parts.

1) Insertion: Each puzzle piece has four notches, close to 5 μm width and 10 μm long. As part's thickness is 5 μm, assembly of two pieces requires to insert perpendicularly (figure 22).

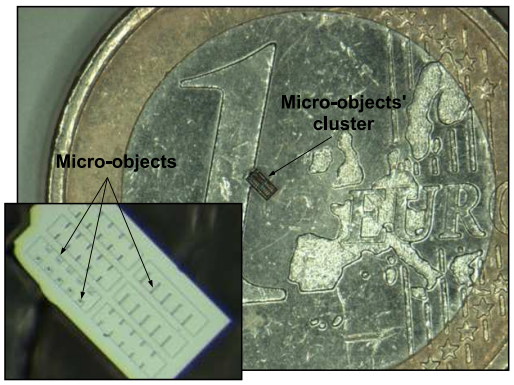

Fig. 21. Micro-objects designed for assembly.

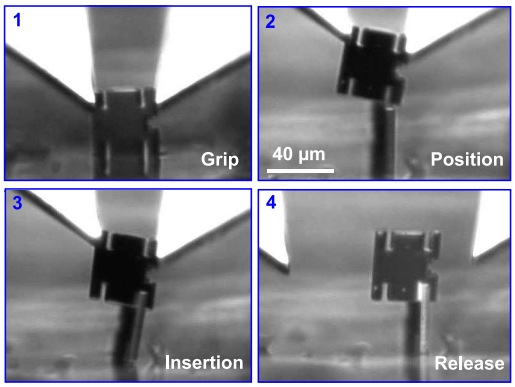

Fig. 22. Insertion assembly.

The first part is gripped and place vertically on the substrate. The second part is taken vertically too perpendiculary to the first one (step 1). Then two puzzle pieces are ready to be assembled. Then the second part is gripped, and is accurately positioned above the first part (step 2). Assembly clearance is very small and evaluated to 200 nm by SEM measurement and accuracy can be made up by substrate compliance. Indeed, compliance of adhesive substrate allows small rotative motion of the first part thus insertion is easily performed without any fine orientation of the gripper (step 3). When insertion is complete, microgripper is opened to release assembled part (step 4). This last operation can failed when adhesive effects between gripper and puzzle piece are stronger than between both puzzle pieces. In fact, the part stay sticked on the end-effector and opening the gripper disassemble the micro-product. Consequently, the trajectory proposed on section II is used to induce a reliable release.

2) Reversible Assembly: The second assembly benchmark requires more steps and more accuracy. Both mechanical parts are different but have the same square shape of 40 μm side. The first part have a small key joint with a T shape on one side. The second part have a T shaped imprint in center of the square (figure 23). To perform assembly, the key must be inserted in the imprint and then a lateral motion of the second part locks the assembly. This benchmark is inspired from Dechev et al [20].

This benchmark has been tested with our robotic structure

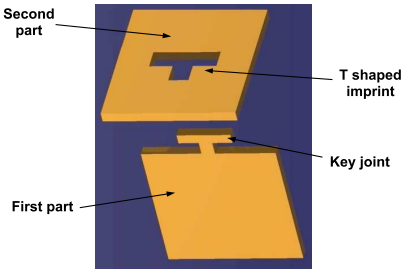

Fig. 23. Lock joint design.

(figure 24). Parts' orientation is very important, especially for the relative orientation between both micro-objects. The first part is set vertically on the substrate. The gripper is used to grip and align the second part above the key (step 1). When the key is in the imprint (visible on the vertical view), a vertical motion puts the key in the hole (step 2). Finally a lateral motion locks the key and the assembly is performed (step 3).

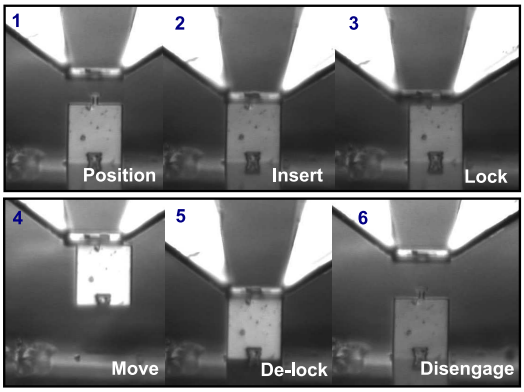

Fig. 24. Reversible assembly.

After locking motion, the 3D microproduct realized can be extracted from the substrate and moved to another place (step 4). Moreover the major interest of this kind of assembly is the possibility to disassemble it. To perform it, motions are repeated on opposite way: a lateral motion to unlock the key (step 5) and a vertical motion to disengage the key from the imprint (step 6). Several cycles of assembly-disassembly have been tested.

3) Analysis of the reliability: In order to show the reliability of our method, numerous pick and place operations have been performed in teleoperation and in an automatic cycle. The tests have been done on a silicon micro-objects whose dimensions are $5 \times 10 \times 20\,\mu m^3$. The objective of the pick and place operation is to grasp the object placed on the substrate, to move it along $100\,\mu m$ and to release it on the substrate. To evaluate the reliability, the success rate of the pick and place operations and the time cycle have been measured.

First, tests have been done in teleoperation. The operator see the lateral view and the vertical view on two screens. He controls the trajectories and the gripper movements with

a joystick without force feedback. 60 operations have been done. The time cycle stays always between 3 and 4 seconds. Secondly, tests have been done in an automatic cycle without force and position feedback. The pick and place trajectory was repeated 60 times and the time cycle was 1.8 seconds.

In both tests, the reliability reaches 100%. As only some articles in the litterature quote the reliability of micromanipulation methods, it is quite difficult to compare this value with other works. However, tests of the reliabilty of microhandling strategies have been presented in [22], [23]. Both tests have been done on polystyrene spheres whose diameter is $50\,\mu m$. The success rate was between 51% and 67% on around 100 tests in [22] and was between 74% and 95% on 60 tests in [23]. Consequently, our method allows a higher reliability on smaller objects which represents a significant contribution.

V. Conclusion

This paper has drawn an overviwe of the scientific works of FEMTO-ST institute in 'microassembly'. It deals with the tridimensional assembly of objects whose typical size is from 10 microns to 400 microns. We have especially focused on the automation of micro-assembly based on several principles. Closed loop control based on micro-vision has been studied and applied on the fully automatic assembly of several 400 microns objects. Force control has been also analyzed and is used for optical Microsystems assembly. At least, open loop trajectories of 40 microns objects with a throughput of 1800 unit per hour have been achieved. Scientific and technological aspects and industrial relevance have been presented

VI. Acknowledgment

These works have been supported by the French National Agency (ANR) under NANOROL contract ANR-07-ROBO-0003: Nanoanalyse for micromanipulate, and PRONOMIA Contract ANR No. 05-BLAN-0325-01, the European Union under HYDROMEL contract NMP2-CT-2006-026622 : Hybrid ultra precision manufacturing process based on positional- and self-assembly for complex micro-products, FAB2ASM contract FoF.NMP.2012-3 : Efficient and Precise 3D Integration of Heterogeneous Microsystems from Fabrication to Assembly, and by the Franche-Comte region under the MIAAMI Project and NEMO/Marie-Curie. Authors would like to thank C. Gorecki and S. Bargiel, from the MN2S depart. fo FEMTO-ST for their contribution on MOEMS assembly.

References

[1] Andrew I. Comport, Member, Eric Marchand, Muriel Pressigout, and François Chaumette. Real-time markerless tracking for augmented reality: The virtual visual servoing framework. *IEEE Transactions on Visualization and Computer Graphics*, 12(4):615–628, 2006.

[2] J. Agnus, P. Nectoux, and N. Chaillet. Overview of microgrippers and design of a micromanipulation station based on mmoc microgripper. In *IEEE International Symposium on Computational Intelligence in Robotics and Automation, CIRA, Finland*, 2005.

[3] Yu Zhou and Bradley J. Nelson. Calibration of a parametric model of an optical microscope. *Optical Engeenering*, 38(12):1989–1995, 1999.

[4] Mehdi Ammi and Antoine Ferreira. Haptically generated paths of an afm-based nanomanipulator using potential fields. In *Proceedings of the 2004 IEEE Nano*, Munich, Germany, august 2004.

[5] Michael Figl, Christopher Ede, Johann Hummel, Felix Wanschitz, Rolf Ewers, Helmar Bergmann, and Wolfgang Birkfellner. A fully automated calibration method for an optical see-through head-mounted operating microscope with variable zoom and focus. *IEEE TRANSACTIONS ON MEDICAL IMAGING*, Vol. 24, N 11:1492–1499, 2005.

[6] Brahim Tamadazte, Sounkalo Dembélé, and Nadine Le Fort-Piat. A multiscale calibration of a photon video microscope for visual servo control: Application to micromanipulation. In *ROSE 2008 - IEEE International Workshop on Robotic and Sensors Environments, Ottawa, Canada, 17-18 October*, 2008.

[7] Kanty Rabenorosoa, Cédric Clévy, Philippe Lutz, Michael Gauthier, and Patrick Rougeot. Measurement of pull-off force for planar contact at the microscale. *Micro Nano Letters*, 4:148 –154, 2009.

[8] M. Rakotondrabe C. Clévy and N. Chaillet, editors. *Signal Measurement and Estimation Techniques for Micro and Nanotechnology*. Springer, To appear in 2011.

[9] S.Bargiel J. P. Mascaro P. Lutz K. Rabenorosoa, C. Clvy and C. Gorecki. Modular and reconfigurable 3d micro-optical benches : Concept, validation, and characterization. In *nternational Manufacturing Science & Ingineering Conference*, 2011.

[10] C. Clvy C. Gorecki S. Bargiel, K. Rabenorosoa and P. Lutz. owards micro-assembly of hybrid moems components on reconfigurable silicon free-space micro-optical bench. *Journal of Micromechanics and Microengineering*, 20(4), 2010.

[11] K. Rabenorosoa, C. Clévy, and P. Lutz. Active force control for robotic micro-assembly: Application to guiding tasks. In *IEEE ICRA, International Conference on Robotics and Automation*, May 2010.

[12] K. Rabenorosoa, C. Clévy, Q. Chen, and P. Lutz. Study of forces during micro-assembly tasks using two-sensing-finger grippers. *IEEE/ASME Transactions on Mechatronics*, Submitted.

[13] D.S. Haliyo and S. Regnier. Manipulation of micro-objects using adhesion forces and dynamical effects. In *Proceedings of ICRA/IEEE Internation Conferenace on Robotics and Automation*, May 2002.

[14] J. Dejeu, M. Gauthier, P. Rougeot, and W. Boireau. Adhesion forces controlled by chemical self-assembly and ph, application to robotic microhandling. *ACS Applied Materials and Interfaces*, 1(9):1966–1973, 2009.

[15] Jérôme Dejeu, Patrick Rougeot, Michaël Gauthier, and Wilfrid Boireau. Reduction of micro-object's using chemical functionalisation. *Micronanoletters*, 2009.

[16] J. Dejeu, P. Rougeot, M. Gauthier, and W. Boireau. Robotic microhandling controlled by chemical self-assembly. In *Proc. of the IEEE/RSJ Int. Conf. on Robotics and Intelligent Systems*, St. Louis, Missouri, USA, Oct. 2009.

[17] J. Dejeu, M. Benchelany, L. Philippe, P. Rougeot, J. Michler, and M. Gauthier. Reducing the adhesion between surfaces using surface structuring with ps latex particle,. *ACS Applied Materials & Interfaces*, 2(6), Juin 2010.

[18] David Heriban, Joël Agnus, Jean-René Coudevylle, Michaël Gauthier, and Nicolas Chaillet. Design of silicon finger tips for a moc (microrobot on chip) microgripper. In *Proc. of the Int. Workshop on Topica Meeting on Microfactories (TMMF05)*, Tsukuba, Japan, October 2005.

[19] J. Agnus, D. Hriban, M. Gauthier, and V. Ptrini. Silicon end-effectors for microgripping tasks. *Precision Engineering*, 2009.

[20] N. Dechev, J. K. Mills, and W. L. Cleghorn. Mechanical fastener designs for use in the microassembly of 3d microstructures. In *Proceedings of ASME IMECE 2004*, 2004.

[21] D. Hriban, J. Agnus, V. Ptrini, and M. Gauthier. Mechanical detethering technique for silicon mems etched with drie process. *Journal of Micromechanics and Microengineering*, 19(5):055011, 2009.

[22] M. Gauthier, B. Lopez-Walle, and C. Clévy. Comparison between micro-objects manipulations in dry and liquid mediums. In *proc. of CIRA'05*, June 2005.

[23] Mélanie Dafflon, Benoit Lorent, and Reymond Clavel. A micromanipulation setup for comparative tests of microgrippers. In *International Symposium on Robotics (ISR)*, 2006.